Structural Eng./Earthquake Eng. Vol. 12, No. 3 · No. 4, 79s—93s, January 1996
Japan Society of Civil Engineers (J. Struct. Mech. Earthquake Eng. No. 531/ I —34)

SPECTRAL CHARACTERISTICS OF STRONG GROUND MOTIONS IN TERMS OF PEAK VALUES

Makoto KAMIYAMA[1]

[1]Member of JSCE, Dr. of Eng., Professor, Dept. of Civil Eng., Tohoku Institute of Technology
(35-1 Yagiyama Kasumicho Taihaku-ku, Sendai 982, Japan)

A theoretical relation between the characteristic periods and peak values of strong ground motions is derived based on random-vibration theory. The relation, summarized as a simple form of theorem, is analogous to the one between period and amplitude of a harmonic motion. The theorem leads to the bounded prediction of central periods whose upper and lower limit values are dependent only on peak acceleration, peak velocity and peak displacement. Following the confirmation of its validity in comparison with observed strong-motion records, the theorem is further expanded to theoretically scale acceleration, velocity and displacement spectra in seismic source area.

Key Words : *strong-motion peaks, central period, random-vibration theory, spectra*

1. INTRODUCTION

Peak values of strong ground motions have been conveniently used in earthquake engineering because of their simplicity. Of the peak values of acceleration, velocity and displacement motions, the first one has received attention from engineers as the most meaningful value in earthquake-resistant design, coupled with inertia forces acting on structures. In view of earthquake damage to structures, however, peak velocity might be similarly significant because it is not only associated with motion energy but also is related closely to strain content. In addition, peak displacement can also become crucial in some engineering problems such as the sloshing of fluid materials during earthquakes. Thus various peak values of strong motions are important depending on different phenomena of various systems. Therefore a unified assessment of peak acceleration, peak velocity and peak displacement is desirable and reasonable in light of the fact that they are interrelated. Many researchers throughout the world have so far studied characteristics of peak acceleration, but most of them did not necessarily pay sufficient attention to the other two kinds of peaks: peak velocity and peak displacement except some studies[1), 2), 3), 4)]. Kamiyama et al.[5)] recently made a semi-empirical analysis of the three kinds of peaks, based on a theoretical faulting source model and a statistical method, in line with the point of view described above. This paper was in part motivated to make a good use of their empirical attenuation relations of peak acceleration, peak velocity and peak displacement.

As is well known, acceleration, velocity and displacement motions are interrelated by means of differential and/or integral operations through their spectral content. Since peak values reflect somewhat spectral content of their motions, the characteristic periods giving peak acceleration, peak velocity and peak displacement might have a close relation with the peak values. In other words, there is a possibility that we obtain spectral information of acceleration, velocity and displacement motions merely by investigating the interrelationships of the three kinds of peaks. Frequency characteristics of strong ground motions play an important role in causing earthquake damage as well as their peaks, so the interrelationships between frequency content and peak values are expected to give a significant insight to earthquake-resistant design procedure. Sawada et al.[6)] investigated statistically the relation between the ratio of peak acceleration to peak velocity and spectral content of acceleration motion without giving theoretical considerations. As opposed to their study, this paper places emphasis on theoretical analyses leading to more

comprehensive relations between peak values and frequency content. The main aims of this paper are: to derive a theoretical relation between the peak values and their characteristic periods; to confirm the validity of the theoretical relation in comparison with the corresponding relation in observed strong ground motions; to obtain the dependence of central periods of acceleration, velocity and displacement spectra on earthquake magnitude by use of an empirical attenuation rule of peak values; and to give a scaling law of strong motion spectra in terms of peak values.

2. THEORETICAL RELATIONS BETWEEN CENTRAL PERIODS AND PEAK VALUES OF STRONG GROUND MOTIONS

(1) Derivation of a theorem

In this section, we derive a theorem describing the relation between the peak values and central periods based on random-vibration theory.

Now let $f(t)$ and $F(f)$ be a time history of strong ground motions and its Fourier transform, respectively. From the Parseval theorem, we then get

$$rms[f(t)]_T = \sqrt{\frac{1}{T}\int_{-\infty}^{\infty} |F(f)|^2 df} \tag{1}$$

where $rms[\ ]_T$ means the rms value of $f(t)$ for the duration T, $|\ |$ is the absolute value and t and f are time and frequency each.

Eq.(1) leads to the following expressions for acceleration motion $a(t)$ and velocity motion $v(t)$:

$$rms[a(t)]_{T_a} = \sqrt{\frac{1}{T_a}\int_{-\infty}^{\infty} |A(f)|^2 df} \tag{2}$$

$$rms[v(t)]_{T_v} = \sqrt{\frac{1}{T_v}\int_{-\infty}^{\infty} |V(f)|^2 df} \tag{3}$$

In Eqs. (2) and (3), $A(f)$ and $V(f)$ are, respectively, the Fourier transforms of acceleration and velocity motions and Ta and Tv mean each the durations for both motions.

According to the differential or integral operations, $A(f)$ and $V(f)$ are connected with each other as follows:

$$2\pi f\,|V(f)| = |A(f)| \tag{4}$$

In order to consider a characteristic period of the velocity motion, we here deal with the second order moment m_v^2 and zero-th order moment m_v^0 of the energy spectrum $|V(f)|^2$. These values can be defined in the frequency domain and given using Eq.(4) as

$$m_v^2 = 2\pi \int_{-\infty}^{\infty} (2\pi f)^2 |V(f)|^2 df = 2\pi \int_{-\infty}^{\infty} |A(f)|^2 df \tag{5}$$

$$m_v^0 = 2\pi \int_{-\infty}^{\infty} |V(f)|^2 df \tag{6}$$

By the use of Eqs. (2) and (3), m_v^2 and m_v^0 become respectively

$$m_v^2 = 2\pi T_a \{rms[a(t)]_{T_a}\}^2 \tag{7}$$

$$m_v^0 = 2\pi T_v \{rms[v(t)]_{T_v}\}^2 \tag{8}$$

We now designate the central frequency of $V(f)$ as $\bar{f}_v$. The central frequency $\bar{f}_v$ is expressed as the square root of the ratio of m_v^2 to m_v^0 and using Eqs. (7) and (8) we obtain

$$2\pi \bar{f}_v = \sqrt{m_v^2 / m_v^0} = \{rms[a(t)]_{T_a} / rms[v(t)]_{T_v}\}\sqrt{T_a / T_v} \tag{9}$$

In addition to the central frequency of $V(f)$, we further introduce the central frequency $\bar{f}_a$ of $A(f)$. Then both central frequencies are connected with the durations T_v and T_a through the numbers of extrema N_v and N_a [7]:

$$T_v = N_v / (2\bar{f}_v) \tag{10}$$

$$T_a = N_a / (2\bar{f}_a) \tag{11}$$

On the other hand, the method of random-vibration theory gives a relation between the peak value, rms value and number of extrema for a random motion [7), 8)]. That is, the expected value of peak velocity $v_{\max}$ is written as

$$E[v_{\max}] = rms[v(t)]_{T_v}\{\sqrt{2\ln N_v} + \gamma / \sqrt{2\ln N_v}\} \tag{12}$$

where $E[\ ]$ means the expected value and γ is the Euler number.

Similarly for acceleration motion,

$$E[a_{\max}] = rms[a(t)]_{T_a}\{\sqrt{2\ln N_a} + \gamma / \sqrt{2\ln N_a}\} \tag{13}$$

where $a_{\max}$ is the peak value of acceleration motion $a(t)$.

When we consider the duration satisfying the condition of $N_a = N_v = N$, Eqs. (12) and (13) give the relation

$$E[a_{\max}] / E[v_{\max}] = rms[a(t)]_{T_a} / rms[v(t)]_{T_v} \tag{14}$$

where $T_a = N/(2\bar{f}_a)$ and $T_v = N/(2\bar{f}_v)$.

Finally, the peak ratio $E[a_{max}]/E[v_{max}]$ is expressed by the central frequencies $\bar{f}_a$ and $\bar{f}_v$ from Eqs. (9), (10) and (11) under the condition of $N_a = N_v = N$ as follows:

$$E[a_{max}]/E[v_{max}] = 2\pi\sqrt{\bar{f}_a \bar{f}_v} \tag{15}$$

The above relation is also applied to velocity and displacement motions:

$$E[v_{max}]/E[d_{max}] = 2\pi\sqrt{\bar{f}_v \bar{f}_d} \tag{16}$$

where d_{max} is the peak value of displacement motion and $\bar{f}_d$ is the central frequency of displacement spectrum.

Meanwhile, in the case of a harmonic motion with a frequency f, the amplitudes of acceleration, velocity and displacement motions have the well-known relations[8)]

$$a/v = 2\pi f \tag{17}$$

$$v/d = 2\pi f \tag{18}$$

where a, v and d are the amplitudes of harmonic acceleration, velocity and displacement motions respectively.

A comparison of Eqs. (15) and (16) with Eqs. (17) and (18) shows that the expected peak values of random motions are interrelated in terms of the central frequencies of their spectra similarly to the relation between amplitudes and frequency of a harmonic motion, regarding the harmonic mean of the two relevant central frequencies as an effective frequency of the random motions. The above discussion is summarized in a form of theorem as follows:

Theorem,

Peak acceleration, peak velocity and peak displacement can be operated, as shown in Eqs.(15) and (16), in a similar manner to the acceleration, velocity and displacement amplitudes of a harmonic motion through an effective frequency given by the harmonic mean of the central frequencies for the two neighboring peak parameters.

(2) Bounded central periods of acceleration, velocity and displacement motions

The above theorem does not give a point value of central frequencies, but only the interrelations of them. However, Eq. (4), a differential relation and/or integral relation, gives an inequality $\bar{T}_a \le \bar{T}_v \le \bar{T}_d$ where $\bar{T}_a$, $\bar{T}_v$ and $\bar{T}_d$ are the central periods, respectively, for acceleration, velocity and displacement motions. This inequality can provide a way for specifying the bounds of these central periods in cooperation with the above theorem. In the following, the expected value symbol | | used in Eqs. (15) and (16) is omitted for the sake of simplicity.

Since $\bar{T}_v > 0$, the inequality becomes

$$\bar{T}_a \bar{T}_v \le (\bar{T}_v)^2 \le \bar{T}_v \bar{T}_d \tag{19}$$

With regard to $\bar{T}_a \bar{T}_v$ and $\bar{T}_v \bar{T}_d$ in Eq. (19), both are expressed in terms of the peak values as shown in Eqs. (15) and (16), and then the inequality of Eq. (19) is transformed to

$$2\pi v_{max}/a_{max} \le \bar{T}_v \le 2\pi d_{max}/v_{max} \tag{20}$$

Following the bounded $\bar{T}_v$ in Eq. (20), we can further bound $\bar{T}_a$ and $\bar{T}_d$ as a form of inequality by using Eqs. (15) and (16). The results are

$$2\pi v_{max}^3/(a_{max}^2 d_{max}) \le \bar{T}_a \le 2\pi v_{max}/a_{max} \tag{21}$$

$$2\pi d_{max}/v_{max} \le \bar{T}_d \le 2\pi a_{max} d_{max}^2/v_{max}^3 \tag{22}$$

Eqs. (20), (21) and (22) show that the bounds of central periods for acceleration, velocity and displacement motion spectra can be specified merely in terms of the peak values of their time histories.

(3) Approximate point values of central periods

The bounded values of central periods were expressed in the above, but some engineering judgments frequently require point values of central periods which are given in a simple form as a first approximation. For such a case, the harmonic means of the upper and lower limit values in Eqs.(20), (21) and (22) may be the best choice because they are simply expressed by the peak values. These approximate central periods based on the hatmonic means of the upper and lower limit values are given by

$$\bar{T}_a \approx 2\pi \frac{v_{max}^2}{\sqrt{a_{max}^3 d_{max}}} \tag{23}$$

$$\bar{T}_v \approx 2\pi \sqrt{\frac{d_{max}}{a_{max}}} \tag{24}$$

$$\bar{T}_d \approx 2\pi \frac{\sqrt{a_{max} d_{max}^3}}{v_{max}^2} \tag{25}$$

Eqs.(23), (24) and (25) would be useful for the purpose of simply estimating central periods of acceleration, velocity and displacement motions.

3. VALIDITY OF THE THEOREM BASED ON COMPARISON WITH OBSERVED STRONG-MOTION DATA

In an attempt to establish validity of the above theorem, we here apply it to strong ground motions observed in Japan. **Fig.1** shows, as an example, a set of strong-motion records observed at Hachirogata, Akita Prefecture, during the 1983 Nihonkai-chubu earthquake [9]. The velocity and displacement records in **Fig.1** were numerically obtained from the acceleration record based on the instrumental frequency correction and a band pass filter. The band pass filter, proposed by Iai et al.[10] as a standard filter for accelerograms obtained by the SMAC accelerometer, has a flat part ranging from about 0.08 sec to about 4.2 sec. In **Fig.1**, peak values of acceleration, velocity and displacement are also given along with their time histories. The Fourier spectra of these records are shown in **Figs.2** (1), (2) and (3) together with the central period bounds which were obtained from the peak values using Eqs. (20), (21) and (22).

It is seen in **Figs.2** (1), (2) and (3) that the theoretical bounds of central periods due to the peak values move toward longer periods in accordance with the spectral characteristics of acceleration, velocity and displacement. Judging from the spectral features, these theoretical bounds seem to correspond to the shift of the central periods of acceleration, velocity and displacement spectra. Another example of such a comparison is given in **Fig. 3** and **Figs.4** (1), (2) and (3) for some other strong-motion records[11] which were observed at Kushiro during the 1973 Nemuro-hanto-oki earthquake and have a different spectral feature from the Hachirogata records. **Fig.3** and **Figs. 4** (1), (2) and (3) also show a similar shift of the theoretical bounds reflecting the central periods of spectra. **Fig.1** through **Figs.4** (1), (2) and (3) are representative examples of comparisons on the basis of spectral figure. We further obtained central periods both due to spectra and peak values from many strong ground motions observed in Japan. Both central periods are plotted, as a scatter diagram, in **Figs.5**, **6** and **7** separately for acceleration, velocity and displacement. The strong ground motions used in these figures are the same as the data set of the author's past study[12]. In **Figs.5**, **6** and **7**, the central periods due to the observed spectra plotted in the horizontal axis were obtained by the central period of spectra as defined

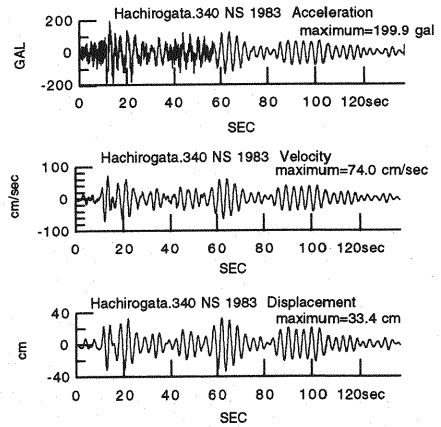

Fig.1 Strong ground motion records at Hachirogata during the 1983 Nihonkai-chubu earthquake.

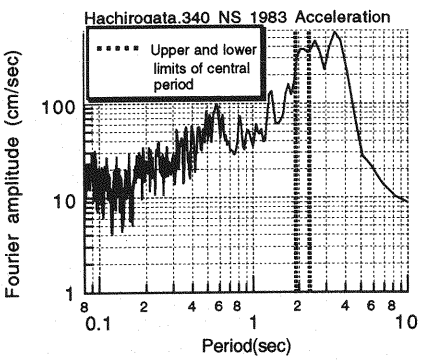

Fig.2 (1) Fourier spectrum of acceleration record at Hachirogata.

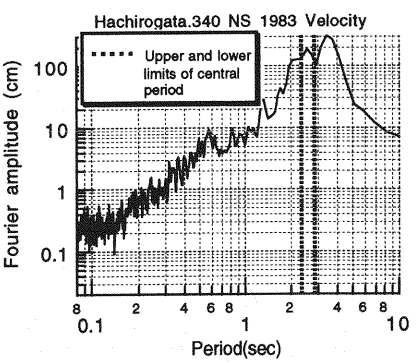

Fig.2 (2) Fourier spectrum of veocity record at Hachirogata.

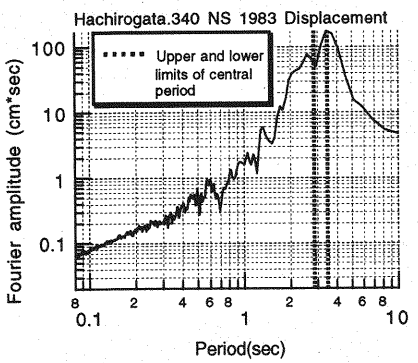

Fig.2 (3) Fourier spectrum of displacement record at Hachirogata.

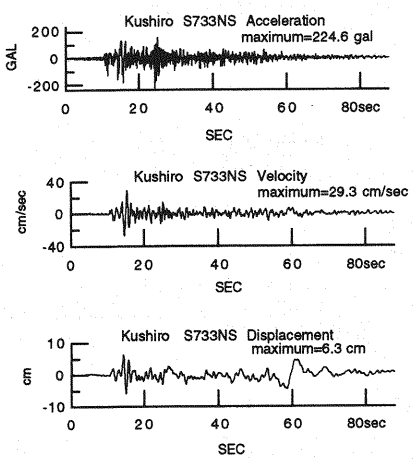

Fig.3 Strong ground motion records at Kushiro during the 1973 Nemuro-hanto oki earthquake.

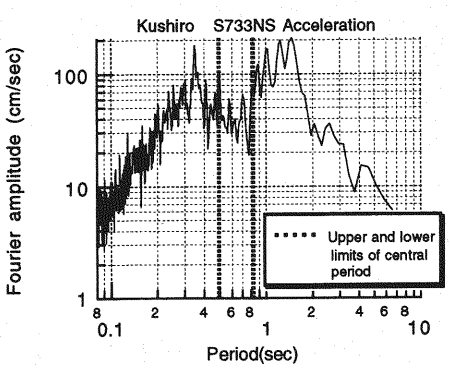

Fig.4(1) Fourier spectrum of acceleration record at Kushiro.

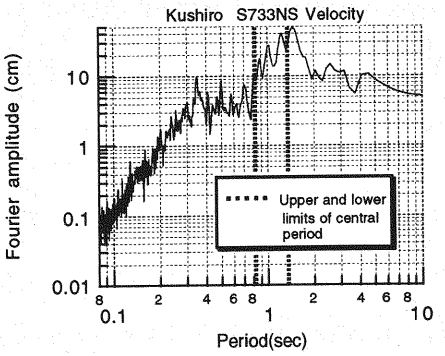

Fig.4(2) Fourier spectrum of velocity record at Kushiro.

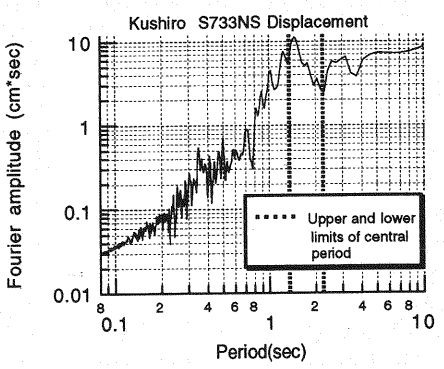

Fig.4(3) Fourier spectrum of displacement record at Kushiro.

in Eq.(9) while the central periods due to the peak values plotted in the vertical axis were estimated as the upper and lower limits of the bounded central periods given in Eqs.(20), (21) and (22). **Figs.5, 6** and **7** systematically demonstrate that the theoretical bounds due to peak values almost include the central periods by spectra. Namely, the 1-to-1 lines ,which denote that the two types of central periods perfectly coincide, almost fall within a range between the upper and lower limits in each comparison of acceleration, velocity and displacement. Thus the theoretical bounds provide, as a whole, a reasonable estimate of central periods, but there seems to be less valid for velocity and displacement in comparison with the case of acceleration. The less validity for velocity anf displacemenr is considered to be due to the long-period problem of their numerically obtained records.

4. DEPENDENCE OF PREDOMINANT PERIODS OF STRONG GROUND MOTIONS ON EARTHQUAKE MAGNITUDE

According to recently developed theories on faulting source model, frequency content, especially predominant periods of strong ground motions are expected to have a close relation with earthquake size. In the past, frequency content of strong ground motions has been discussed mainly based on spectra of actually obtained strong-motion records. However, since spectral features are generally influenced by various factors such as seismic source, propagation path of waves and local soils, it has not necessarily been possible to correctly extract frequency content due solely to seismic source. In addition, the small number of strong-motion records obtained at rock sites in an epicentral area has made it difficult to scrutinize the dependence of frequency content on earthquake size. The theorem presented in the preceding section is applied here to investigate the dependence of predominant periods of acceleration, velocity and displacement motions on earthquake magnitude. In this section, we assume that the central periods presented in Eqs.(20), (21) and (22) are equivalent to the predominant periods which are usually dealt with as the peak-period in spectra.

As shown in Eqs.(20), (21) and (22), to obtain a magnitude-dependent predominant period, we require a consistent attenuation relation of peak acceleration, peak velocity and peak displacement depending on earthquake magnitude. Kamiyama et al.[5] derived semi-empirically an attenuation relation of the three kinds of peak values in terms of earthquake magnitude, hypocentral distance and local soil conditions, using both of a theoretical faulting source model and 357 strong-motion records observed in Japan. The results are:

$$a_{\max}(i,M,r) = 518.9 \times AMP_i(a) \qquad (26)$$
$$for \quad (r \le 10^{0.014+0.218M})$$

$$a_{\max}(i,M,r) = 547.6 \times 10^{0.358M-1.64\log_{10} r} \times AMP_i(a) \qquad (27)$$
$$for \quad (r > 10^{0.014+0.218M})$$

$$v_{\max}(i,M,r) = 2.879 \times 10^{0.153M} \times AMP_i(v) \qquad (28)$$
$$for \quad (r \le 10^{0.014+0.218M})$$

$$v_{\max}(i,M,r) = 3.036 \times 10^{0.511M-1.64\log_{10} r} \times AMP_i(v) \qquad (29)$$
$$for \quad (r > 10^{0.014+0.218M})$$

$$d_{\max}(i,M,r) = 0.189 \times 10^{0.236M} \times AMP_i(d) \qquad (30)$$
$$for \quad (r \le 10^{0.014+0.218M})$$

$$d_{\max}(i,M,r) = 0.200 \times 10^{0.594M-1.64\log_{10} r} \times AMP_i(d) \qquad (31)$$
$$for \quad (r > 10^{0.014+0.218M})$$

where $a_{\max}$ is peak horizontal acceleration in cm/sec^2, $v_{\max}$ is peak horizontal velocity in cm/sec,

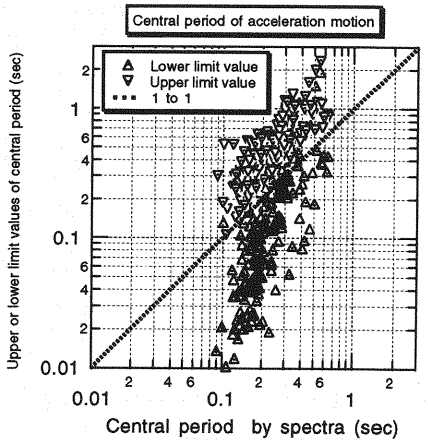

Fig.5 Comparison between central period due to observed spectra and central period due to peak values for acceleration motions.

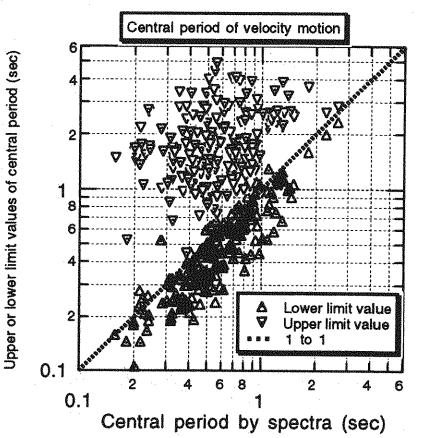

Fig.6 Comparison between central period due to observed spectra and central period due to peak values for velocity motions.

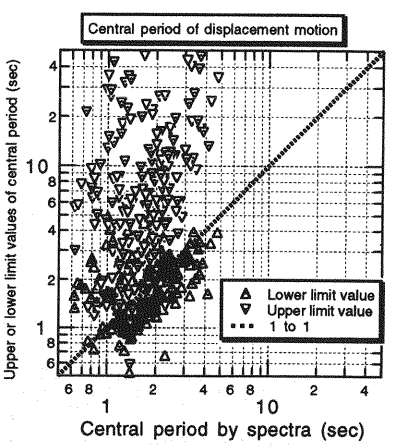

Fig.7 Comparison between central period due to observed spectra and central period due to peak values for displacement motions.

d_{max} is peak horizontal displacement in cm, i is the number for identifying the observation sites used in the Kamiyama et al. analysis, M is the JMA earthquake magnitude, and r is the hypocentral distance in km.

As expressed in Eqs.(26) through (31), their attenuation relations have a constant level in value in a fault area whose length is assumed to be equivalent to the radius of a circular fault and dependent on earthquake magnitude. The terms $AMP_i(a)$, $AMP_i(v)$ and $AMP_i(d)$ in Eqs.(26) through (31) mean an amplification factor due to local soils without which the peak values on seismic bed rock can be estimated. The seismic bed rock in this case is regarded as a rock physically equivalent to the reference site employed by their analysis; its S-wave velocity is in the range of 1 to 2 km/sec. Using Eqs.(26), (28) and (30) with the condition of $AMP_i(a) = AMP_i(v) = AMP_i(d) = 1$ as well as Eqs.(20) thorough (22), we made an attempt to estimate predominant periods for acceleration, velocity and displacement motions on seismic bed rock in the fault area. **Fig.8** shows the estimated predominant periods dependent on earthquake magnitude. In the figure, the bounds of predominant periods for acceleration, velocity and displacement are plotted along with their harmonic means by Eqs.(23), (24) and (25). **Fig.8** gives a characteristic feature that predominant periods of seismic motions become longer with increasing earthquake magnitude. Note in the case of velocity and displacement motions that their predominant periods are influenced largely by the period range of the band pass filter used for the computation of their numerical records. Thus the predominant periods of velocity and displacement motions here may be somewhat inaccurate in comparison with acceleration which is less affected by the period range. With regard to the magnitude-dependent predominant periods of seismic motions at rock sites in a fault area, few systematic studies have been so far carried out except for the Seed et al. study[13]. Seed et al. investigated systematically predominant periods of acceleration motions observed at rock sites in a fault area during earthquakes in California, the U.S. They presented a figure to show predominant periods of acceleration motions depending on earthquake magnitude and epicentral distance. In **Fig.8**, predominant periods of acceleration motions picked up from the figure by Seed et al. are plotted as solid circles. The Seed el al. results fall within the bound of this study, giving a similar trend of increase with earthquake magnitude. This is considered another evidence representing the validity of the present theorem with respect to the relations between the peak values and predominant periods.

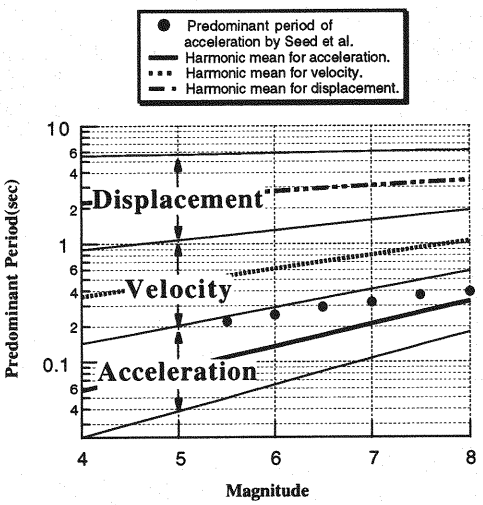

Fig.8 Dependence of predominant periods of acceleration, velocity and displacement at rock site in fault area on earthquake magnitude.

5. THEORETICAL SPECTRA OF STRONG MOTIONS ASSOCIATED WITH PEAK VALUES

In this section, we shall make an attempt to derive a scaling law of acceleration, velocity and displacement spectra, using and expanding the relations between time and frequency domains which resulted in the above theorem of central periods. Random-vibration theory, for example, Eq.(12) provides the fact that peak value of motions is connected with their spectral content through the Parseval theorem. This means that we can inversely determine spectral amplitudes of motions in terms of peak values. In order to perform such an inverse determination of spectra, we need a basic structure of spectral features for acceleration, velocity and displacement motions.

As for spectral structures of strong ground motions which are due only to source parameters without the effects of path and local soils, a variety of proposals has been made based on theoretical faulting source models and/or observations. Among them, the ω square model, proposed by Aki[14], has received supports from many researchers as effective for predicting earthquake motion spectra. The acceleration source spectrum $A(T)$ due to the model is simply expressed by

$$A(T) = M_o(2\pi/T)^2/\{1+(T_0/T)^2\} \qquad (32)$$

where M_o is the seismic moment, T_0 the corner period determined by the source parameters such as the stress drop and seismic moment and T period.

The acceleration spectrum by Eq.(32) has two asymptotic lines that intersect at the corner period T_0. The spectral amplitudes in the long-period range are proportional to T^{-2} while those in the short period range have a constant level: $M_0(2\pi/T_0)^2$. The spectral shape is sketched in **Fig.9** where another corner period T_f, proposed and referred to as f_{max} by Hanks[15], is attached. In **Fig.9**, velocity and displacement spectra derived from Eq.(32) are also shown with arbitrary scales of spectral amplitudes. Although its corner periods T_0 and T_f are associated with source parameters differently depending on researchers, the ω square model has been used to develop more sophisticated source spectra. For example, the specific barrier model, which was implemented by Papageorgiou and Aki[16] to describe faulting on a heterogeneous plane, has been developed on the assumption that some sub-cracks generate spectral amplitudes related to the ω square model. In consideration of such a wide applicability, we also here use the ω square model as a base for building strong-motion spectra in terms of peak values. The spectral shapes shown in **Fig.9** provide no conspicuous predominant periods whereas acceleration, velocity and displacement spectra are respectively dominant in the short-period, intermediate-period and long-period ranges. In addition, they are a kind of idealized spectra with no effects of heterogeneous faulting process and other complicated source factors which are usually involved in observed motion spectra. We herein modify the spectral shapes so that their spectral amplitudes are compatible with observed ones and contain the central period bounds given in the preceding section.

In viewing the period-dependent features, each spectrum in **Fig.9** may be approximated by a combination of four linear variations with period T: as an example of acceleration, its spectral amplitudes are proportional to T, T^0, T^{-1} and T^{-2} ranging from the shortest to the longest period parts which are divided by the periods $\hat{T}_a$, $\hat{T}_{av}$ and $\hat{T}_{vd}$. **Fig.10** shows such linearly-varying spectrum of acceleration as well as velocity and displacement spectra which are similarly approximated and scaled in an arbitrary manner for their spectral amplitudes. Though being impossible to strictly determine the

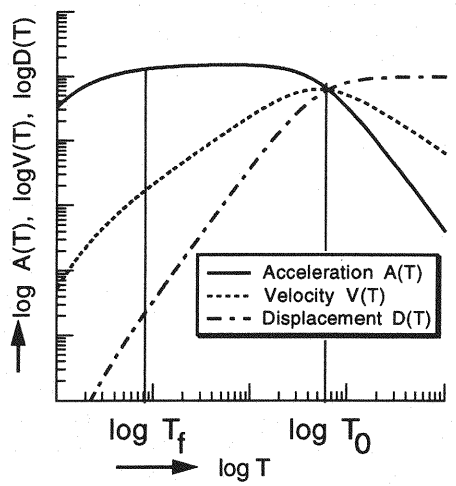

Fig.9 A schematic figure of acceleration, velocity and displacement spectra due to the ω square model.

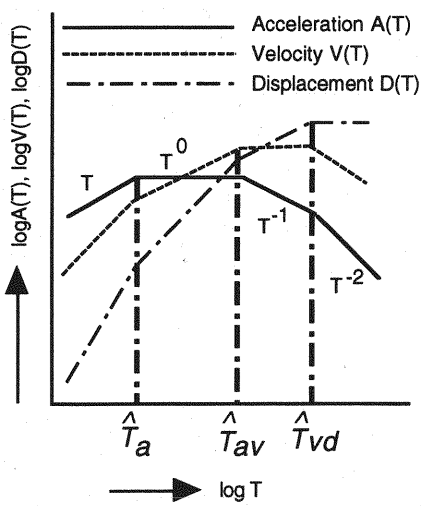

Fig.10 A schematic figure of linearly approximated spectra for acceleration, velocity and displacement.

central periods from the spectral shapes in **Fig.10**, each flat part may be interpreted to correspond to some predominant period range as a first approximation. We thus assume that the lower and upper limit periods of each flat part are equivalent to the two boundary values for the inequalities of central periods given previously in terms of peak values. That is, the intersection periods $\hat{T}_a$, $\hat{T}_{av}$ and $\hat{T}_{vd}$ are given by

$$\hat{T}_a = 2\pi v_{\max}{}^3 / (a_{\max}{}^2 \times d_{\max}) \quad (33)$$

$$\hat{T}_{av} = 2\pi v_{\max} / a_{\max} \quad (34)$$

$$\hat{T}_{vd} = 2\pi d_{\max} / v_{\max} \quad (35)$$

The above models of spectra use corner periods diffrent from the original ω square model, so we will hereafter call them "linear-model-spectra." Their basic structures are determined from the information of the peak values and the random-vibration theory such as Eqs.(12) and (13). According to Eq.(13), the expected value of peak acceleration is given by

$$E[a_{\max}\} = \frac{\sqrt{2\ln N_a} + \gamma / \sqrt{2\ln N_a}}{\sqrt{N_a \overline{T}_a}} \times 2\sqrt{\int_0^\infty |A(f)|^2 \, df} \quad (36)$$

where N_a is the number of extrema, $\overline{T}_a$ the central period, γ the Euler constant and $A(f)$ the spectrum of acceleration.

Of the terms of the right-hand side in Eq.(36), $\overline{T}_a$ can be approximated by the harmonic mean of $\hat{T}_a$ and $\hat{T}_{av}$ while the spectrum $A(f)$ was already set up for its basic structure. Furthermore, the extrema number N_a will be determined by some information of the duration for acceleration motion as expressed in Eq.(11). The duration of acceleration motion is associated with the rupture time of faulting in seismic source, traveling time and so on, but the time length of main acceleration motion may depend principally on the rupture time of faulting source. This means that the duration T_a of main acceleration motion is determined by l/V where l is the characteristic length of the fault and V is the velocity of rupture propagation on the fault plane. As for the characteristic length of seismic fault, several proposals have been made empirically or theoretically, being related with earthquake magnitude. For example, Kamiyama et al.[5] obtained empirically the following earthquake magnitude-dependent radius of a circular fault in the process of deriving the attenuation laws of peak strong-motions presented in Eqs.(26) through (31):

$$l = 1.03 \times 10^{0.218M} \quad (37)$$

where l is the radius of a circular fault in km and M is the JMA earthquake magnitude.

In this paper, we use the Kamiyama et al. empirical radius for a characteristic length of fault because our target spectra in a fault area are scaled in

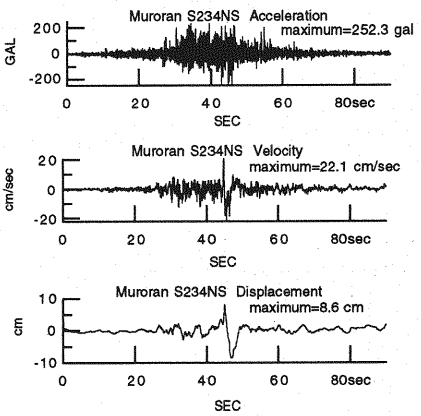

Fig.11 (1) Strong-motion records obtained at Muroran during the 1968 Tokachi-oki earthquake.

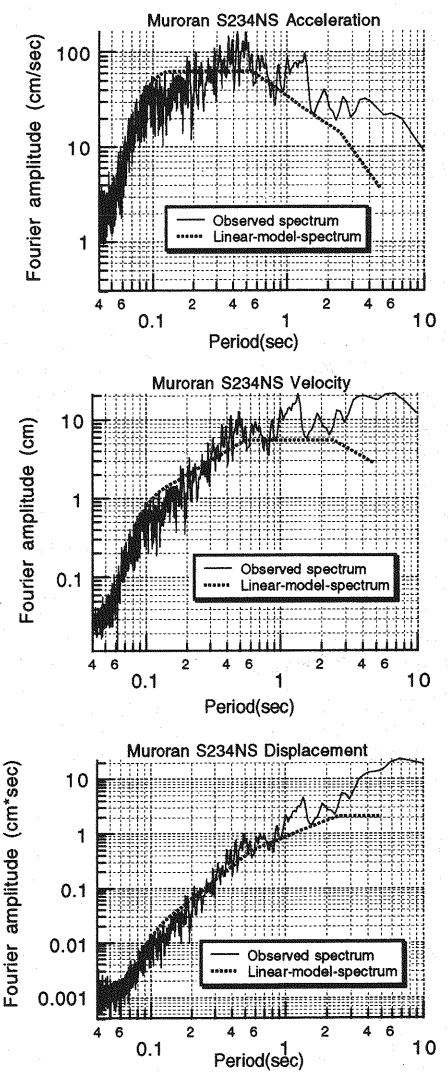

Fig.11 (2) Fourier spectra of the Muroran records and linear-model-spectra estimated by this study's method.

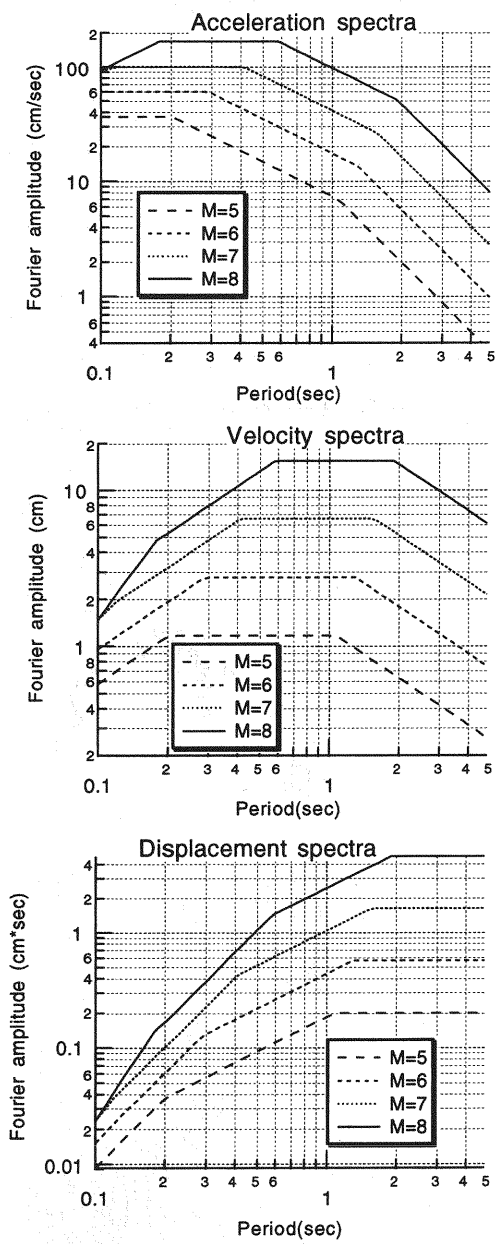

Fig.12 Acceleration, velocity and displacement spectra in seismic source area estimated by the linear-model - spectrum method with the aid of the Kamiyama et al. empirical law of strong-motion peaks.

terms of their attenuation laws of peak acceleration, peak velocity and peak displacement. On the other hand, the velocity of rupture propagation V was herein assumed to be 2.52 km/sec in reference to the Geller study[17]. Using the duration of motion determined by the above values of l and V, the extrema number N_a in Eq.(36) is finally given by

$$N_a = 0.82 \times 10^{0.218M} / \overline{T}_a \tag{38}$$

It follows from the above discussion that we can obtain the acceleration spectrum $A(f)$ by inversely solving Eq.(36). Note that the velocity spectrum $V(f)$ and displacement spectrum $D(f)$ are similarly obtained by the use of random-vibration theory applied to peak velocity and peak displacement.

In order to confirm the adequacy of how to determine the linear-model-spectra outlined above, we compared them with real spectra obtained from strong-motion records. **Figs. 11** (1) and (2) show one example of such comparison. In **Fig.11** (1), a set of strong-motion records which include acceleration, velocity and displacement motions at Muroran during the 1968 Tokachi-oki earthquake[18] are shown with their peak values. The Fourier spectra for their main motion parts are shown as solid lines in **Fig.11**(2). In **Fig.11**(2), dotted spectra indicate the linear-model-spectra estimated only from the information of peak acceleration, peak velocity, peak displacement and earthquake magnitude. We can see in **Fig.11**(2) that the linear-model-spectra follow relatively well the corresponding real spectra,. This means that the method for constructing the linear-model-spectra can be applied to some extent to predict strong-motion spectra. Based on such a confirmation of its validity, the linear-model-spectra method was further coupled with the Kamiyama et al. attenuation laws of the peak values: Eqs. (26) through (31). This was attempted because a unified prediction of acceleration, velocity and displacement spectra in seismic source area has been rarely performed in the past studies.

Using Eqs.(26), (28) and (30) with the condition of $AMP_i(a) = AMP_i(v) = AMP_i(d) = 1$, acceleration, velocity and displacement spectra in seismic area were estimated as shown in **Fig.12**. These spectra are scaled only by earthquake magnitude because they are predicted with no effects of path and local soils. It is clear in **Fig.12** that spectral amplitudes of acceleration, velocity and displacement dominate in different period ranges depending on earthquake size. The next problem is to confirm validity of

these predicted spectra. For such a purpose, we need strong-motion records which were obtained at a rock site near seismic source because the predicted spectra were provided under the condition of no effects of path and local soils. Nearly satisfying such a condition of observation site, there exists a small number of strong-motion records, all obtained during recent earthquakes in the U.S. Among them are the Santa Cruz record in the 1989 Loma Prieta erthquake[19] and the Pacoima dam down-stream record in the 1994 Northridge earthquake[20]. The former was obtained at a limestone site with an epicentral distance of 16 km while the latter recorded at a hard rock with an epicentral distance of 18 km. These strong-motion records are thus considered to nearly satisfy the required conditions. **Figs.13**(1) and (2) show two horizontal components' records for the Santa Cruz site and **Figs.14** (1) and (2) are those for the Pacoima down-stream site. They are all composed of acceleration, velocity and displacement records. Note here that these records were directly cited from the reports of the California Strong Motion Instrumentation Program(CSMIP) in which the accelerometer and the data process method are quite different from those used for the strong-motion records in this study. In particular, the band-pass filter for CSMIP is much broader in the long period range, so the displacement motions which are mainly determined by long period characteristics might have less reliability of comparison. The Fourier spectra obtained from the main parts of these records are shown in **Figs.15** and **16**.

With the information of a magnitude of 7.0 for the 1989 Loma Prieta earthquake and 6.7 for the 1994 Northridge earthquake, we can theoretically estimate strong-motion spectra in the seismic source area for both events not only using Eqs.(26), (28) and (30) restricted as $AMP_i(a,v,d)=1$ but also using the linear-model-spectrum method. These theoretical estimates of spectra are indicated as thick solid lines in **Figs.15** and **16**. Comparisons of the theoretical spectra with the observed ones in **Figs.15** and **16** show that the method of the linear-model-spectrum gives a relatively good prediction within the period range between about 0.1 sec and about 3 sec. Since comparisons in the long period range are less reliable as stated above, the degree of agreement in **Figs.15** and **16** may be acceptable in view of the fact that the linear-model-spectrum method uses only information of earthquake magnitude without any other detailed source parameters related to faulting process. This indicates that the theorem of central periods presented in this study has a wide scope of

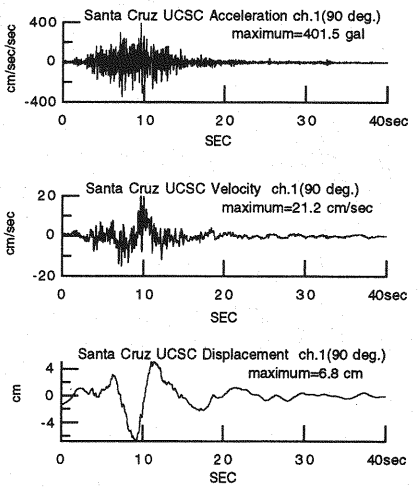

Fig.13 (1) Strong-motion records in the 90 degree horizontal direction at the Santa Cruz site during the 1989 Loma Prieta earthquake.

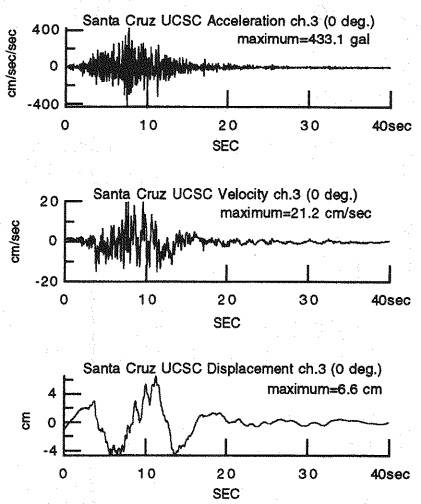

Fig.13 (2) Strong-motion records in the 0 degree horizontal direction at the Santa Cruz site during the 1989 Loma Prieta earthquake.

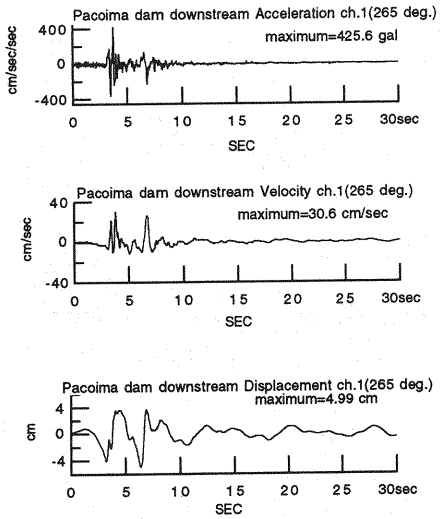

Fig.14 (1) Strong-motion records in the 265 degree horizontal direction at the Pacoima down-stream site during the 1994 Northridge earthquake.

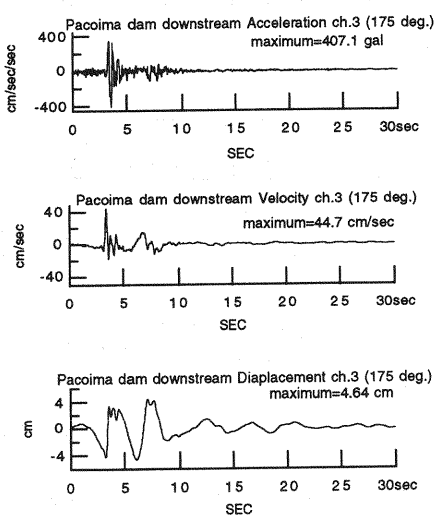

Fig.14 (2) Strong-motion records in the 175 degree horizontal direction at the Pacoima down-stream site during the 1994 Northridge earthquake.

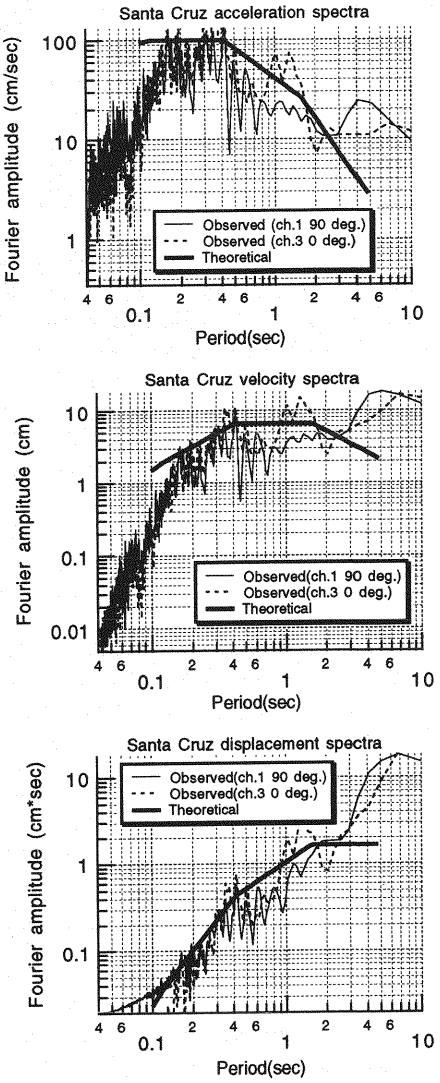

Fig.15 Fourier spectra for the Santa Cruz records and theoretical spectra estimated due to the linear-model-spectrum method.

applications in collaboration with strong-motion peaks which are comparatively available for data acquisition.

6. SUMMARY AND CONCLUSIONS

The principal motive of this study is that the three kinds of strong-motion peaks: peak acceleration, peak velocity and peak displacement should be used systematically in light of their equal importance in earthquake engineering. In the past, a unified estimate of the three kinds of peaks has not necessarily been performed with sufficient attention in both the time domain and frequency domain. This study has focused on the interrelationships of them with emphasis on the frequency domain because frequency characteristics of strong motions play a deterministic part in causing earthquake damages as well as motion amplitudes. The derived theorem of frequency content related with peak values of seismic motions has a quite simple and somewhat elegant form analogous to a harmonic motion. At the same time, the theoretical relations of frequency content are widely applicable to various problems in earthquake engineering because of their simplicity. In this study, it was shown as an example for their applications how predominant periods and spectra of acceleration, velocity and displacement motions are dependent on earthquake magnitude with the aid of an empirical expression of strong-motion peaks. The main concluding remarks derived from this study are:

1) The central periods of seismic acceleration, velocity and displacement motions are related with the motions peaks similarly to the relations between the amplitudes and periods of a harmonic motion as expressed in Eqs.(15) and (16). The harmonic mean of central periods for the two neighboring peak parameters plays the same role as the frequency of a harmonic motion. These relations were obtained using random-vibration theory and summarized as a theorem in this study.

2) According to the theorem, the bounds of central periods of acceleration, velocity and displacement motions were specified as a form of inequalities whose upper and lower limits are determined in terms of peak values. The inequalities are expressed in Eqs.(20) through (22).

3) The theorem and bounds of central periods were derived under the condition of the equal number of extrema for the two neighboring random motions among acceleration, velocity and displacement. In order to establish the validity of the theorem and bounds on the basis of such a condition, the central periods due to the theoretical

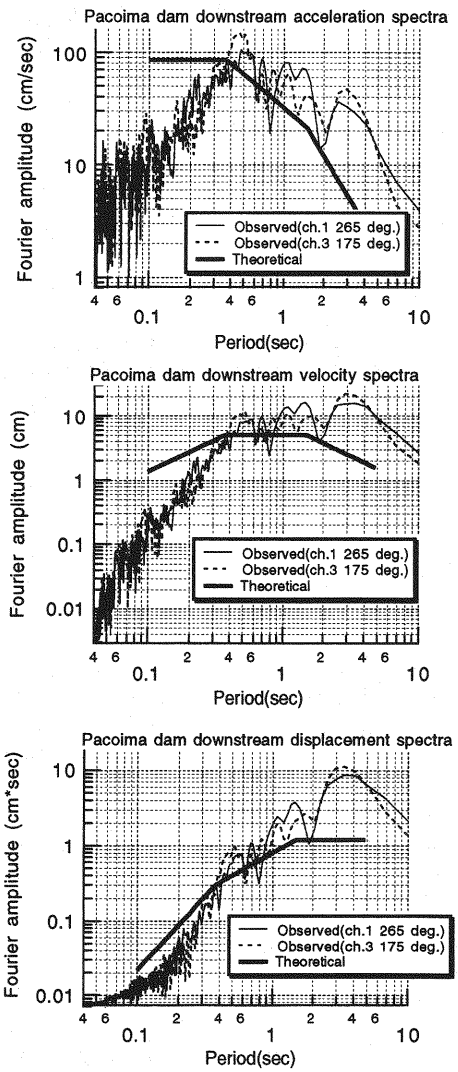

Fig.16 Fourier spectra for the Pacoima down-stream records and theoretical spectra estimated due to the linear-model-spectrum method.

relations were compared with observed ones. The comparisons showed that the bounds of central periods due to the theoretical relations almost include the central periods from observed spectra. However, the comparisons for velocity and displacement were less valid because their peak values were numerically obtained through a period-limited band pass filter.

4) The theoretical relations were applied to estimate predominant periods of acceleration, velocity and displacement motions in an epicentral

area which are not due to local soils and propagation path of waves but to only source parameters. The estimate was carried out by the use of an empirical law of strong-motion peaks. The results of predominant period for acceleration were found to be relatively compatible with the observational study by Seed et al.

5) Similarly to the prediction of predominant periods due solely to seismic source, a unified estimate of spectra for acceleration, velocity and displacement motions in an epicentral area were attempted expanding the theorem to spectral content of motions. In the process for deriving the basic structure of spectra, the ω-square model was used and modified so that the central periods resulting from the theorem are explicitly involved. As a result, a simplified spectrum dependent only on strong-motion peaks, called here "linear-model-spectrum", was derived and further applied to predict acceleration, velocity and displacement spectra in a seismic source area as shown in **Fig.12**. The adequacy of such a prediction of spectra was confirmed in comparison with two representatives of actually observed spectra at rock sites near epicenters of earthquakes in the U.S.

Although the linear-model-spectrum method presented here gives a simplified prediction of spectra relatively compatible to the observed within the limited period range, it seems to have an insufficient estimate in longer periods and therefore less reliable estimates for velocity and displacementt spectra. This is due to the over-simplification of the method as well as the peak values of velocity and displacement motions used in this paper which were obtained in a period-limited manner to avoid numerical errors. In addition, spectral prediction for velocity and displacement should be coupled with seismic source theory because spectral amplitudes in loger periods are more dependent on such a theory. Accordingly, more sophisticated spectral shape reflecting complicated faulting process of seismic source is needed to enhance the applicability of the theorem presented in this paper while velocity or displacement records reliable in much longer periods are indispensable for future studies.

REFERENCES

1) Trifunac, M. D.: Preliminary analysis of the peaks of strong earthquake ground motion- dependence of peaks on earthquake magnitude, epicentral distance and recording site conditions, *Bull Seism. Soc. Am.*, Vol.66, No.1, pp.189-219, 1978.

2) McGuire, R. K.: Seismic ground motion parameter relations, *Journal of the Geotechnical Engineering Division*, Proc.ASCE, Vol.104, No.GT4, pp.481-490. 1978.

3) Boore, D. M., Joyner, W. B., Oliver, A. A. and Page, R. A.: Peak acceleration, velocity and displacement from strong motion record, *Bull Seism. Soc. Am.*, Vol. No.1, pp.305-321, 1980.

4) Kawashima, K., Aizawa, K. and Takahashi, K.: Attenuation of peak ground motion and absolute acceleration response spectra, *Proc. of Eighth World Conf. on earthquake Eng.*, Vol.2, pp.257-264, 1984.

5) Kamiyama, M., O'Rourke, M. J. and Flores-Berrones, R.: A semi-empirical model of strong-motion peaks with appropriate comparison to the 1989 Loma Prieta, the 1985 Michoacan and the 1971 San Fernando earthquakes, *Structral Eng. and Earthquake Eng.*, Vol.10, No.4, pp.187-197, 1994.

6) Sawada, T., Hirao, K. and Yamamoto, H.: Relation between maximum amplitude ratios(a/v, ad/v^2) and spectral parameters of earthquake ground motion, *Proc. of 10th World Conf. on Earthquake Eng.*, Vol.2, pp.617-622, 1992.

7)Joyner, W. B. and Boore, D. M.: Measurement, characterization and perdition of strong ground motions, *Proc. of Earthquake Engineering and Soil Dynamics II*, GT Div/ASCE, pp.43-102, 1988.

8) Nigam, N. C.: *Introduction to Random Vibrations*, The MIT Press, pp.140-144, 1983.

9) Japan Society of Civil Engineers: *Report on the 1983 Nihonkai-Chubu Earthquake*, pp.49-70, 1986 (in Japanese).

10) Iai, S., Kurata, E. and Tsuchida, H.: Digitization and correction of strong-motion accelerigrams, *Technical Note of Port and Harbor Research Institute*, No.286, pp.5-56, 1978 (in Japanese).

11) Kurata, E., Ishizaki, T. and Tsuchida, H.: Annual Report on Strong-Motion Earthquake Records in Japanese Ports (1973), *Technical Note of Port and Harbor Research Institute*, No.181, pp.45-68, 1974.

12) Kamiyama, M. and Yanagisawa, E.: A statistical model for estimating response spectra of strong earthquake ground motions with emphasis on local soil conditions, *Soils and Foundations*, Vol.26, No.2, pp.16-32, 1986.

13)Seed, H. B., Idriss, I. M. and Kiefer, F. W.: Characteristics of rock motions during earthquakes, *Journal of Soil Mechanics and Foundations*, ASCE, pp.1199-1218, 1969.

14) Aki, K.: Scaling law of earthquake source time-function, *Geopgys. J. R. astr. Soc.*, Vol.31, pp.3-25, 1972.

15) Hanks, T. C.: f_{max}, *Bull Seism. Soc. Am.*, Vol.72, pp.1867-1879, 1982.

16) Papageorgiou, A. S. and Aki. K.: A specific barrier model for the quantitative description of inhomogeneous faulting and the prediction of strong ground motion, Part I and II, *Bull. Seism. Soc. Am.*, Vol.73, pp.693-722, pp.953-978, 1983.

17) Geller, R. J.: Scaling relations for earthquake source parameters and magnitudes, *Bull. Seism. Soc. Am.*, Vol.66, pp.1501-1523, 1976.

18) Tuschida, T. Kurata, E. and Sudo, K.: Strong-Motion Earthquake Records of the1968 Tokachi-Oki Earthquake and its Aftershocks, *Technical Note of Port and Harbor Research Institute*, No.80, pp.1-476, 1969.
19) Huang, M. J., Cao, T. Q., Vetter. U. R. and Shakal, A. F.: Second Interim Set of CSMIP Processed Strong-Motion Records from the Santa Cruz Mountains(Loma Prieata) Earthquake of 17 October 1989, *Report No. OSMS* 90-01, California Strong Motion Instrumentation Program, 1990.
20) Darragh, R., Cao, T., Cramer, C., Huang, M. and Shakal, A.: Processed CSMIP Strong-Motion Records from the Northridge, California Earthquake of January 17, 1994: *Release No.1, Report OSMS* 94-06A, California Strong Motion Instrumentation Program, 1994.

(Received January 5, 1995)